Band-gap engineering with HfS_xSe_{2-x}

Christof Gaiser, Thorsten Zandt, Alica Krapf, Ralf Serverin, Christoph Janowitz, and Recardo Manzke
Institut für Physik, Humboldt Universität zu Berlin, Invalidenstrasse 110, 10115 Berlin, Germany
(Received 9 January 2003; revised manuscript received 24 September 2003; published 17 February 2004)

The band gaps of HfS_2 (1.96 eV) and $HfSe_2$ (1.13 eV) cover the range of ideal band gaps for photovoltaic applications which is for a single-junction cell about 1.45 eV and for a two-junction cell about 1.1 eV and 1.8 eV. Additionally, in favor of applications the transition-metal dichalcogenides have a strong tendency to grow as thin films due to their quasi-two-dimensional character. Employing the chemical vapor transport method, single crystals of this ternary semiconductor were grown with nine different compositions. They were characterized in detail by low-energy electron diffraction, Laue diffraction, and energy dispersive x-ray analysis. In addition the absorption at room temperature was measured, revealing an absorption coefficient $\alpha(h\nu)$ that is remarkably high for an indirect semiconductor. The determined band gaps of HfS_xSe_{2-x} show a nearly linear dependence on x, which is perfect for band-gap engineering. Furthermore, in the gap an exponential behavior of $\alpha(h\nu)$ is observed, which could be interpreted as an Urbach tail.

DOI: 10.1103/PhysRevB.69.075205 PACS number(s): 78.40.Fy, 71.35.Cc, 81.10.Bk

I. INTRODUCTION

The semiconducting dichalcogenides investigated in this paper are binary and ternary compounds of the group-IVb transition metal Hf and chalcogenides S and Se. These materials have a 1T structure with octahedral coordination of the chalcogenides by the metal atom [see Fig. 1(a)]. The bonding between the dichalcogenide layers is van der Waals like. For this reason they can be regarded as quasi two dimensional. In the plane strong covalent-ionic bonds dominate. The configuration of the transition metal Hf is $5d^26s^2$ and that of the chalcogenides S and Se is $3s^23p^4$ and $4s^24p^4$, respectively. The four valence electrons of the transition metal are transferred to the two chalcogenide atoms to fill their valence shell (d_0 configuration):

$$M_{d^2s^2} + 2C_{s^2p^4} \rightarrow M^{4+}_{d^0s^0} + 2C^{2-}_{s^2p^6}. \quad (1)$$

The p orbitals of the chalcogenides and the s/p orbitals of the metal form bonding σ and antibonding σ^* bands, resulting in a gap between 5 and 10 eV. Within this gap the d states of the transition metal are located. These are split due to the ligand field and a trigonal distortion. The d_{xz} and d_{yz} orbitals are repelled by p_x and p_y orbitals of the chalcogenides and are therefore energetically on the highest level. The same holds for the $d_{x^2-y^2}$ and d_{xy} orbitals repelled by the p_z chalcogenide orbitals. The most interesting orbital with the lowest energy is that with d_{z^2} symmetry. This is empty and forms the lowest conduction band. For the Hf dichalcogenide the p-d interactions are weak, yielding semiconductors with quite large energy gaps. Figure 1(b) shows the resulting band model, proposed by Friend and Yoffe.[1] In the present work, the p-d energy gap variation of a complete series of the ternary compounds HfS_xSe_{2-x} has been studied systematically.

II. EXPERIMENTS

The crystals were all grown by chemical vapor transport (CVT),[4,5] a powerful method to grow perfect single crystals. Most of the crystals were produced by iodine transport and one was grown using Se itself as transport agent. The powder of Se, S, and I had a purity of 99.999%. The purity of Hf powder given by the producer, due to a natural contamination with Zr, was 99.98%. Energy dispersive x-ray (EDX) measurements revealed a higher amount of 0.5% Zr, but due to the similar electronic structure of Zr and Hf, we do not expect a measurable influence on the absorption spectrum. These substances were put into a sealed quartz ampoule together with 5 mg/cm^3 iodine. The ampoule was placed in the temperature gradient of a four-zone furnace (with two buffer zones to avoid thermal disturbance from outside). Table I lists the grown crystals and their properties.

The reflectance R/R_0 was measured using an Al mirror for the normalization and the transmittance T/T_0 was normalized by a direct light beam. These measurements were taken with a prism monochromator (Carl Zeiss Jena) and a computer using a high-precision digital voltmeter (Schlumberger technologies 7071). The thickness of the crystals was determined with an electron microscope (Cambridge Instruments S360) [see Fig. 2(b)], and the stoichiometry was measured by EDX (Rontec EDR 288). For a qualitative determi-

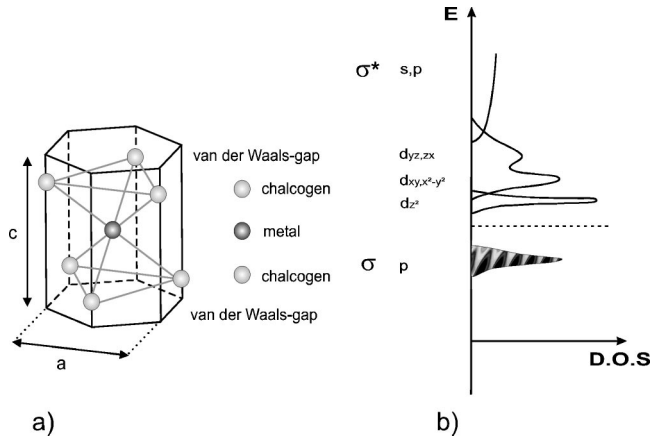

FIG. 1. (a) 1T structure. (b) Band model after Friend and Yoffe (Ref. 1) for the group-IVB transition-metal dichalcogenides.

TABLE I. List of the single crystals grown by CVT.

HfS_xSe_{2-x}	$\pm x$	Zone temp. (°C) T_{cold}	T_{warm}	Transport agent	Thickness (μm$\pm$1%)	Color
$x=2$	0	840	900	I	4.8	Red
$x=1.85$	0,03	835	900	I	6.7	Red
$x=1.55$	0,07	750	950	Se	3.4	Brown
$x=1.3$	0,06	850	900	I	5.0	Blue
$x=1.2$	0,05	830	900	I (Nb doped)	7,5	Blue metallic
$x=0.95$	0,05	840	900	I	12.4	Blue
$x=0.7$	0,07	850	900	I	11.3	Blue
$x=0.4$	0,04	830	900	I	12.2	Metallic
$x=0.2$	0,04	810	900	I	3.1	Metallic
$x=0$	0	810	900	I	17.0	Metallic

nation of the structure low-energy electron diffraction (LEED) (VG Microtech RVL 900) [Fig. 2(b)] and Laue diffraction patterns were taken.

III. RESULTS AND DISCUSSION

The equation describing the wavelength-dependent transmission is given by

$$T(\lambda)=\frac{T}{T_0}\simeq\frac{[1-R(\lambda)]^2e^{-\alpha(\lambda)d}}{1-R(\lambda)^2e^{-2\alpha(\lambda)d}}. \quad (2)$$

For sufficiently high values of αd like in our case (see Ref. 2) Eq. (2) can be simplified to

$$\alpha(\lambda)\simeq\frac{1}{d}\{-\ln T(\lambda)+2\ln[1-R(\lambda)]\}. \quad (3)$$

This is the usual dependence of the absorption coefficient $\alpha(\lambda)$ on the reflection index $R(\lambda)$, the transmission $T(\lambda)$, and the thickness d of the crystals. For all crystals the transmittance and reflectance was measured [see, for example, Fig. 3(a)]. We found for all compounds that R is constant in the regarded energy range, which has been also observed for HfS_2 and ZrS_2 by Terashima and Imai.[6] From Eq. (3) the absorption spectra can be calculated. Figure 3(b) shows the results for our samples. We see that an increase of the relative amount of sulphide shifts the absorption edge to higher energy. The band gap was determined by analyzing the energy dependence of the absorption coefficient $\alpha(h\nu)$ (Ref. 7):

$$\alpha(h\nu)=\text{const}\times f_B\int_0^{-h\nu-E_g\pm E_p}N(E_i)N(E_f)dE_i. \quad (4)$$

$N(E_i)$ and $N(E_f)$ are the density of the initial and final states, respectively, and f_B is the Einstein-Bose function that accounts for the distribution of the involved phonons with energy E_p. For isotropic structures the density of states (DOS) behaves like

$$N(E_i)\sim\sqrt{|E_i|},\quad N(E_f)\sim\sqrt{(h\nu-E_g\pm E_p+E_i)}. \quad (5)$$

Solving Eq. (4) by employing Eq. (5), the absorption coefficient for $T=$const becomes

$$\alpha(h\nu)\sim(h\nu-E_g\pm E_p)^2. \quad (6)$$

Due to the extreme anisotropic structure of the samples, it is very common[8] to assume a two-dimensional (2D) DOS as

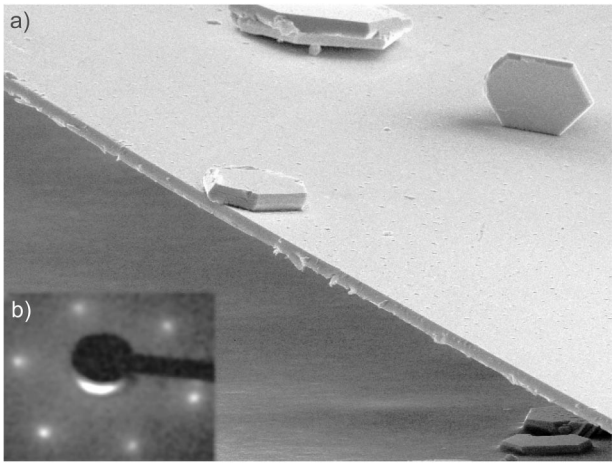

FIG. 2. (a) Image of $HfS_{1.3}Se_{0.7}$ taken by an electron microscope. (b) LEED pattern of $HfS_{0.95}Se_{1.05}$ at $E=121$ eV.

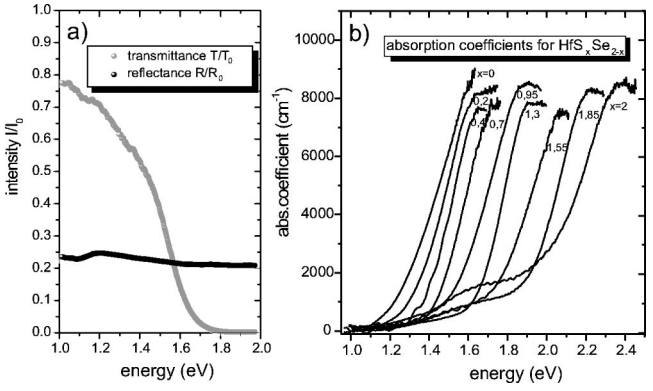

FIG. 3. (a) The transmittance and reflectance of $HfS_{1.3}Se_{0.7}$. The reflectance reveals a nearly constant behavior. (b) Energy-dependent absorption of HfS_xSe_{2-x} for the whole concentration range $0\leqslant x\leqslant 2$.

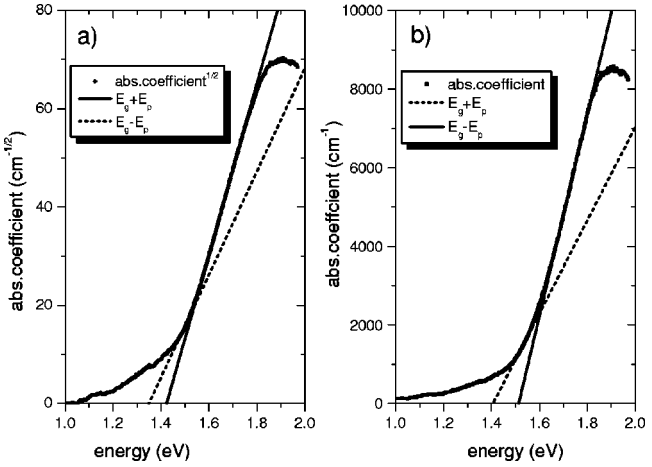

FIG. 4. Example for the determination of the band gap of $HfS_{0.95}Se_{1.05}$ in the (a) three-dimensional ($\sim\alpha^{1/2}$) and (b) two-dimensional ($\sim\alpha$) cases.

discussed in Ref. 9: $N(E_i)=C_1$ and $N(E_f)=C_2$. With Eq. (4) the absorption coefficient then results in

$$\alpha(h\nu)\sim(h\nu-E_g\pm E_p). \tag{7}$$

A characterization of the dimensionality of these crystals is rather difficult.

In Fig. 4 the methods for a determination of the band gap are given. The onset for the phonon absorption for both cases was observed behind the structure which is displayed in detail in Fig. 7 below. A linear dependence in the band-gap region is visible. The phonon energies related to the process are listed for all models in Table II. Infrared-spectroscopy data[3] verified a LO phonon at 39.4 meV for HfS_2 and for $HfSe_2$ at 26.7 meV. A comparison with Table II shows that the phonon energies assumed for the band-gap determination seem to be reasonable. Also the tendency to smaller phonon energies form HfS_2 to $HfSe_2$ can be verified by Table II.

As can be seen it is not possible to decide definitely which dimensionality is adequate. Thus more generally we fit $\alpha(h\nu)$ by

$$\alpha(h\nu)\sim(h\nu-E_g\pm E_p)^D. \tag{8}$$

TABLE II. Band gap E_g resulting from the 2D, 3D, and fit models (see text) and the related phonon energies.

HfS_xSe_{2-x}	E_g (eV) and E_p (meV)					
x	2D model		3D model		D_{fit} model	
2	1.93	50	1.80	40	1.87	45
1.85	1.83	50	1.71	40	1.80	40
1.55	1.68	45	1.58	35	1.65	40
1.3	1.59	40	1.51	30	1.58	35
0.95	1.45	40	1.39	30	1.43	35
0.7	1.39	35	1.31	25	1.38	35
0.4	1.31	30	1.23	25	1.30	35
0.2	1.25	35	1.17	25	1.24	30
0	1.18	30	1.10	25	1.15	30

TABLE III. Literature values of E_{gap} for different methods and different crystalline characters and lattice parameters.

HfS_xSe_{2-x}	Single cryst.[a]	Polycryst.[b]	X-ray diff.[c]		
x	E_g (eV) trans.	E_g (eV) diffuse refl.	c(Å)	a(Å)	c/a
0	1.13	~1.10	3.747	6.158	1.643
0.5		~1.30			
1		~1.49	3.694	6.061	1.641
1.5		~1.72			
2	1.96	~1.98	3.630	5.854	1.612

[a]Reference 2.
[b]Reference 10.
[c]Reference 3.

The result is a value of $1\leqslant D\leqslant 2$ that refers to a dimensionality for the DOS between 2 and 3. In Table II the D values are shown for different x.

The absorption data yield for our samples $D=1.24\pm0.09$. This value leads to a dimensionality of the DOS $\sim 2\frac{1}{4}$, i.e., more two than three dimensional. This result is consistent with the electronic structure along the ΓA direction where a very low dispersion in the bands has been observed. It justifies the indication as a quasi-two-dimensional system. Table II collects all band gaps and related phonon energies. Table III gives a comparison with previous diffuse reflectance measurements on polycrystalline samples and transmission data.[2,10] These values exhibit negligible differences which might be explained by their crystalline character. The basic trend of the gaps can be explained by the variation of the electronegativity and the simple band model described above. The c/a ratio as explained in the Introduction determines the position of the d_{z^2} band, the lowest conduction band. The second effect is the main reason for the behavior of the band gap. There is a difference in electronegativity ϵ of the chalcogenides $\epsilon_S>\epsilon_{Se}$. Due to that dependence, HfS_2 is more ionic than $HfSe_2$ and that leads to a greater band gap. Recapitulating these considerations we come to the following conclusion. The nearly linear dependence of the band gaps with x is a result of a linear change in the electronegativity of the chalcogenides. The marginal changes in the c/a ratio (see Table III) have little effect but might be visible in the minor deviation from the otherwise linear dependence of the gaps for $x\gtrsim 1.3$ in Fig. 5(b).

Fong *et al.*[11] have calculated the gap of HfS_2. They found a value of 1.8 eV for a transition from Γ_{2-} to M_{1+}. That corresponds well with the data of Table II.

IV. URBACH EDGE

In the literature all spectra shown for HfS_2 and $HfSe_2$ start in the region of the indirect band gap. But obviously in the case of HfS_2 there exists a clear additional structure in the ''forbidden'' energy range. This was first observed by Urbach on silver halides.[12] More than 50 years after the first observation, a general theoretical model is still missing. But there exist qualitative agreement that the interaction between

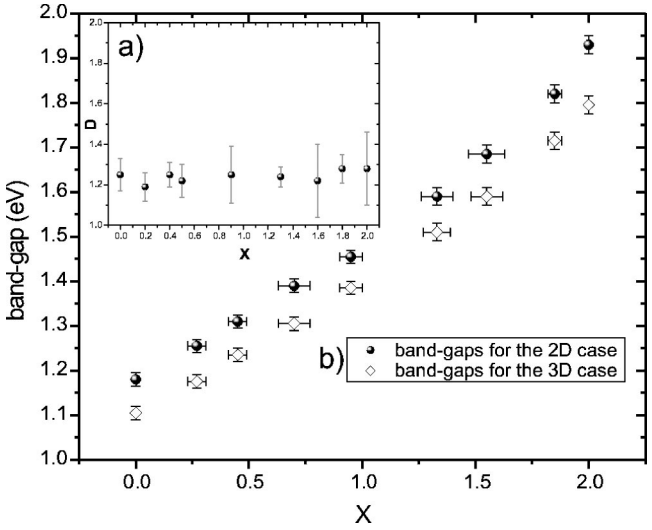

FIG. 5. (a) Band-gap values for all single crystals derived from the two- and three-dimensional models. (b) Dimensionality D of the electronic structure as a function of x due to the fit by Eq. (8).

phonons and excitons should be responsible for this so-called Urbach tail. The main idea here is that the energy of the exciton state is changed due to the lattice deformation Δ by thermal vibrations. Using the deformation potential E_1 this change can be written as

$$\delta E = -E_1 \Delta. \tag{9}$$

The result is an exponential behavior as predicted by Urbach[12]:

$$\alpha(h\nu) \sim \frac{1}{\sqrt{h\nu_0 - h\nu}} \exp\left(-\frac{\sigma}{kT}(h\nu_0 - h\nu)\right), \tag{10}$$

where σ refers to the expression

$$\sigma = \sigma_0 \frac{2kT}{\hbar\omega_p} \tanh \frac{\hbar\omega_p}{2kT}. \tag{11}$$

σ_0 is a specific constant and $\hbar\omega_p$ the energy of the phonons involved. Introducing a quadratic term Toyozawa[13] was able to describe the low-energy absorption tail:

$$\delta E = E_1 \Delta + E_2 \Delta^2, \tag{12}$$

Toyozawa connected the two terms in Eq. (12) to the two parts in the absorption spectra (two-mode model). The linear term, which is responsible for the maximum of the Urbach edge, describes the interaction between the exciton and LA phonons. The absorption near the band maximum is then given by a Gaussian function:

$$\alpha(h\nu) \sim e^{-\tau^2(h\nu_0 - h\nu)^2}. \tag{13}$$

On the other hand, Toyozawa[13] suggested that the absorption at the low-energy tail should be the result of interactions between excitons and LO or TA phonons which will be described by the quadratic term of Eq. (12).

Up to now we have only performed room-temperature measurements of our samples. For a quantitative characterization of the Urbach edge temperature-dependent measurements are essential. Such data would allow one to determine which phonons and excitons are involved in the process. A qualitative fit with the described model is in good agreement with our experimental data [see, for example, Fig. 6(a)]. But there are two other indications for an exciton effect. With a decreasing ratio of S (e.g., lower band-gap) a prominent decrease of the Urbach tail was observed (see Fig. 7). This can be explained by a reduced exciton lifetime with smaller band gap.[15] This behavior is well known from other substances like ternary II-IV compounds.[14] Furthermore, a measurement of a degenerated crystal grown with an amount of Nb as donator was made. Figure 6(b) shows a comparison between an undoped $HfS_{1.3}Se_{0.7}$ crystal and $HfS_{1.2}Se_{0.8}$ doped with Nb. Due to the degeneration, the possibility for excitons is very reduced[16] and is the explanation of the disappearance of the Urbach edge.

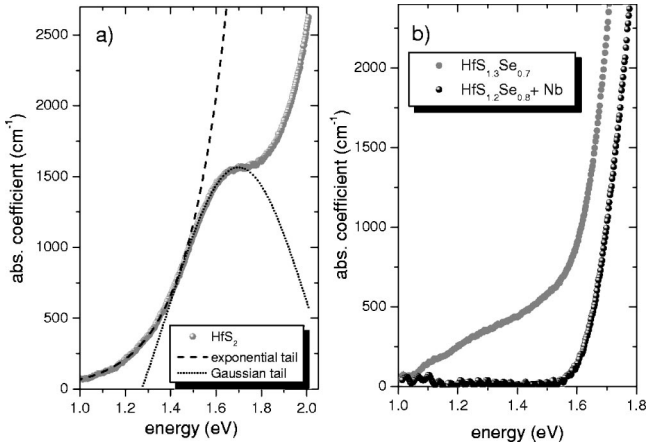

FIG. 6. (a) Fit for HfS_2 following the model of Toyozawa (Ref. 13) by an exponential dependence at the absorption edge and on the top a Gaussian behavior; see the text. (b) Comparison between $HfS_{1.3}Se_{0.7}$ and $HfS_{1.2}Se_{0.8}$ doped with Nb.

V. CONCLUSIONS

The first absorption spectra of ternary HfS_xSe_{2-x} single crystals presented showing that the band gap can be modified

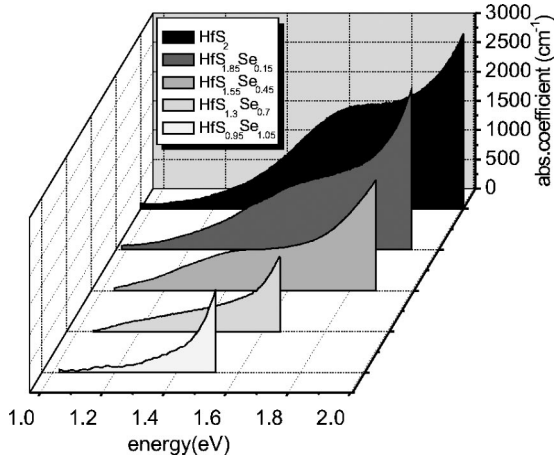

FIG. 7. Behavior of the exponential absorption edge for different stoichiometry.

linearly by changing the parameter x. In principle this behavior can be qualitatively understood within the simple band model of Friend and Yoffe,[1] taking into account the electronegativity and c/a ratio. A fit of the absorption spectra yields an almost two-dimensional electronic structure of these layered materials. The absorption coefficient is rather high for indirect semiconductors. So these materials have optimal optical properties for photovoltaic applications. A structure observed below the absorption edge in particular for sulphur-rich crystals is due to the Urbach edge which disappears for $x \lesssim 0.95$ and also for degenerated crystals.

ACKNOWLEDGMENT

We would like to thank Dr. S. Rogaschewski for the EDX and electron microscope measurements.

[1] R.H. Friend and A.D. Yoffe, Adv. Phys. **36**, 1 (1987).
[2] D.L. Greenaway and R. Nitsche, J. Phys. Chem. Solids **26**, 1445 (1965).
[3] G. Lucovsky, R.M. White, J.A. Benda, and J.F. Revelli, Phys. Rev. B **7**, 3859 (1973).
[4] R. Nitsche, Fortschr. Mineral. **44**, 231 (1967).
[5] H. Schaefer, *Chemische Transportreaktionen* (Verlag Chemie, Weinheim, 1962).
[6] K. Terashima and I. Imai, J. Phys. Soc. Jpn. **59**, 738 (1990).
[7] J.I. Pankove, *Optical Processes in Semiconductors* (Dover, New York, 1971).
[8] P.A. Lee, G. Said, R. Davis, and T.H. Lim, J. Phys. Chem. Solids **30**, 2719 (1969).
[9] R. Fivaz, J. Phys. Chem. Solids **28**, 839 (1967).
[10] L. Brattas and A. Kjekshus, Acta Chem. Scand. **27**, 1290 (1973).
[11] C.Y. Fong, J. Camassel, S. Kohn, and Y.R. Shen, Phys. Rev. B **13**, 5442 (1976).
[12] F. Urbach, Phys. Rev. **92**, 1324 (1953).
[13] Y. Toyozawa, Prog. Theor. Phys. (Kyoto) **22**, 455 (1959).
[14] L. Samuel, Y. Brada, and R. Beserman, Phys. Rev. B **37**, 4671 (1988).
[15] A.R. Beattie and P.T. Landsberg, Proc. R. Soc. London, Ser. A **249**, 16 (1958).
[16] G.D. Mahan, Phys. Rev. **153**, 882 (1967).